Stochastic analysis of unsaturated flow with probabilistic collocation method

Weixuan Li,[1] Zhiming Lu,[2] and Dongxiao Zhang[1,3]

Received 18 October 2008; revised 28 March 2009; accepted 27 May 2009; published 18 August 2009.

[1] In this study, we present an efficient approach, called the probabilistic collocation method (PCM), for uncertainty analysis of flow in unsaturated zones, in which the constitutive relationship between the pressure head and the unsaturated conductivity is assumed to follow the van Genuchten-Mualem model. Spatial variability of soil parameters leads to uncertainty in predicting flow behaviors. The aim is to quantify the uncertainty associated with flow quantities such as the pressure head and the effective saturation. In the proposed approach, input random fields, i.e., the soil parameters, are represented via the Karhunen-Loeve expansion, and the flow quantities are expressed by polynomial chaos expansions (PCEs). The coefficients in the PCEs are determined by solving the equations for a set of carefully selected collocation points in the probability space. To illustrate this approach, we use two-dimensional examples with different input variances and correlation scales and under steady state and transient conditions. We also demonstrate how to deal with multiple-input random parameters. To validate the PCM, we compare the resulting mean and variance of the flow quantities with those from Monte Carlo (MC) simulations. The comparison reveals that the PCM can accurately estimate the flow statistics with a much smaller computational effort than the MC.

Citation: Li, W., Z. Lu, and D. Zhang (2009), Stochastic analysis of unsaturated flow with probabilistic collocation method, *Water Resour. Res.*, *45*, W08425, doi:10.1029/2008WR007530.

1. Introduction

[2] One of the crucial problems in modeling flow and transport in the subsurface is the treatment of uncertainty. Uncertainty may be caused by a number of factors. It is well known that geological media exhibit a high degree of spatial variation over various scales. The properties that control flow and transport in the media, such as permeability and porosity, are also strongly heterogeneous in space. This spatial variability may have a strong impact on fluid flow in the media. Furthermore, these properties are usually measured only at a limited number of locations because of the high cost associated with subsurface measurements. Although the media properties are deterministic, because of the lack of information it is common to treat them as spatially varying random fields, characterized by the statistical moments that are derived from a limited number of measurements. In turn, the partial differential equations governing the subsurface flow in such media become stochastic.

[3] In this study, we consider flow in the heterogeneous vadose zone, which connects the hydrology process above the land surface and the saturated aquifer in the subsurface. The vadose zone also acts as a buffer and passage in the process of pollutants movement from the land surface to groundwater. Because of its important role in determining the pathway of pollutants, the vadose zone has received increasing attention in recent years. Because of the coexistence of water and air phases in this zone, the equation governing the flow in this zone becomes nonlinear; that is, the hydraulic conductivity depends on the pressure head. The nonlinear property coupled with uncertainty leads to a great complexity in the numerical simulations.

[4] Many stochastic approaches have been developed to study the effect of spatial variability on flow in unsaturated zone [*Jury*, 1982; *Yeh et al.*, 1985a, 1985b; *Mantoglou and Gelhar*, 1987; *Mantoglou*, 1992; *Russo*, 1993, 1995; *Tartakovsky et al.*, 1999; *Zhang and Winter*, 1998; *Zhang*, 1999, 2002; *Lu and Zhang*, 2002; *Yang et al.*, 2004]. The Monte Carlo (MC) simulation is the best known and widely used approach in solving stochastic equations. As a statistical sampling approach, the MC is conceptually straightforward and easy to implement. The input random parameters are sampled repeatedly and independently from prescribed distributions, which may be inferred on the basis of the field observations. Then, for each realization (sample) of input random fields, deterministic governing equations are solved to obtain the corresponding realization of output random fields. The required statistical properties, such as the statistical moments and probability density functions, can then be estimated on the basis of these output realizations. A large number of realizations are needed to achieve statistical convergence. Such a procedure usually leads to a high computational cost. As such, the applicability of MC is

[1]Department of Energy and Resources Engineering, College of Engineering, Peking University, Beijing, China.
[2]Earth and Environmental Sciences Division, Los Alamos National Laboratory, Los Alamos, New Mexico, USA.
[3]Also at Sonny Astani Department of Civil and Environmental Engineering and Mork Family Department of Chemical Engineering and Materials Science, University of Southern California, Los Angeles, California, USA.

0043-1397/09/2008WR007530$09.00

often limited to small scale problems. In this study, for the purpose of validating the proposed approach, a large number of MC simulations are used and the results from these MC simulations are considered as the reference.

[5] In this study, a Karhunen-Loeve (KL) expansion based probabilistic collocation method (PCM) is presented for predicting flow in the vadose zone. This approach has been used for stochastic analysis in some fields [*Webster et al.*, 1996; *Tatang et al.*, 1997]. Coupled with the Karhunen-Loeve expansion of the random permeability field, *Li and Zhang* [2007, 2009] applied the PCM method to the simulation of single and multiphase flow in heterogeneous porous media. *Chang and Zhang* [2009] demonstrated the efficiency of PCM in dealing with such problems by comparing it with other approaches. In this approach, the input random field is first expressed as the sum of its mean field and a zero mean perturbation, which is further decomposed by a KL expansion with an infinite number of terms. By truncating the KL series at a finite number of terms, the stochastic model is simplified into finite stochastic dimensions. That is, the random field is represented with a finite set of independent random variables. The steps in implementing the PCM are similar to those of MC in that replicates of the random field are solved deterministically. However, the input replicates are not randomly and equally probably sampled but selected following certain rules and thus referred to as "representations" in this work. The objective of these selection rules is to significantly reduce the number of model simulations required for adequate estimation of output uncertainties, compared to the conventional MC method.

2. Stochastic Differential Equations

[6] Consider flow in unsaturated porous media satisfying the following continuity equation and Darcy's law:

$$B(\mathbf{x},\psi)\frac{\partial\psi(\mathbf{x},t)}{\partial t}+\nabla\cdot\mathbf{q}(\mathbf{x},t)=g(\mathbf{x},t), \tag{1}$$

$$\mathbf{q}(\mathbf{x},t)=-K(\mathbf{x},\psi)\nabla[\psi(\mathbf{x},t)+x_1], \tag{2}$$

subject to initial and boundary conditions:

$$\psi(\mathbf{x},0)=\psi_0(\mathbf{x}),\qquad \mathbf{x}\in D \tag{3}$$

$$\psi(\mathbf{x},t)=H_B(\mathbf{x},t),\qquad \mathbf{x}\in\Gamma_D, \tag{4}$$

$$\mathbf{q}(\mathbf{x},t)\cdot\mathbf{n}=Q(\mathbf{x},t),\qquad \mathbf{x}\in\Gamma_N, \tag{5}$$

where $\mathbf{q}$ is the specific discharge (flux), g is the sink/source term, ψ is the pressure head, x_1 is the elevation, $\psi + x_1$ is the total head, and $K(\mathbf{x}, \psi)$ is the unsaturated hydraulic conductivity, which depends on pressure head ψ. $H_B(\mathbf{x}, t)$ and $Q(\mathbf{x}, t)$ are prescribed pressure head and flux on Dirichlet and Neumann boundary segments, respectively. The specific moisture capacity is defined as $B = d\theta_e/d\psi$, where $\theta_e = \theta - \theta_r$ is the effective water content.

[7] To solve the set of equations described above, one must specify the constitutive relationship between K, B and ψ. Some empirical models have been investigated, including the Gardner-Russo model [*Gardner*, 1958; *Russo*, 1988], the Brooks-Corey model [*Brooks and Corey*, 1964], and the van Genuchten-Mualem model [*van Genuchten*, 1980]. In this study, we adopt the van Genuchten-Mualem model:

$$K(\mathbf{x},t)=K_s(\mathbf{x})\sqrt{S_e(\mathbf{x},t)}\left\{1-[1-S_e^{1/m}(\mathbf{x},t)]^m\right\}^2, \tag{6}$$

$$S_e(\mathbf{x},t)=\{1+[-\alpha(\mathbf{x})\psi(\mathbf{x},t)]^n\}^{-m}, \tag{7}$$

$$B(\mathbf{x},t)=\alpha(\mathbf{x})[n(\mathbf{x})-1](\theta_s-\theta_r)S_e^{1/m}(\mathbf{x},t)[1-S_e^{1/m}(\mathbf{x},t)]^m \tag{8}$$

where K_s is the saturated hydraulic conductivity, $S_e = \theta_e/(\theta_s - \theta_r)$ is the effective saturation, θ_s and θ_r are the respective saturated and residual water content, α is a fitting parameter that is inversely related the mean pore size, $n > 1$ is another fitting parameter that is inversely related to the width of the pore size distribution, and $m = 1 - 1/n$. The dependent variables ψ and S_e can be written as functions of space/time coordinate ($\mathbf{x}$, t), sink/source (g), boundary conditions (H_B, Q), and soil properties (K_s, α, n, θ_s, θ_r): $\psi = \psi(\mathbf{x}, t, g, H_B, Q, K_s, \alpha, n, \theta_s, \theta_r)$, $S_e = S_e(\mathbf{x}, t, g, H_B, Q, K_s, \alpha, n, \theta_s, \theta_r)$.

[8] Uncertainty associated with any argument in ψ and S_e may lead to uncertainty in ψ and S_e. In this study, we assume K_s, α, n to be random fields whereas other arguments are deterministic. They are three input fields in our model. Our purpose is to estimate the statistical properties, i.e., the mean and variance, of the flow quantities such as the pressure and effective saturation, which are the output fields in our model.

3. Representation of the Input Random Fields: Karhunen-Loeve Expansion

[9] The first step of solving stochastic equations is to find a proper way to represent the input and output random fields. In this study, we use Karhunen-Loeve expansion (KL) to represent the input fields, for given covariance functions of the input fields. Since the covariance structures of the output fields are not known in advance, they cannot be expanded using the KL expansion. Instead, they are expressed in a form of Polynomial Chaos Expansion (PCE) as described in section 4.

3.1. Single-Input Random Field

[10] Consider an input random field $U(\mathbf{x}, \omega)$, where $\mathbf{x} \in D$ is the coordinates in the physical domain and $\omega \in \Omega$ denotes the coordinates in the probability space. It is assumed that the mean and covariance function of $U(\mathbf{x}, \omega)$ are known: $\overline{U}(\mathbf{x}) = \langle U(\mathbf{x}, \omega)\rangle$, $C_U(\mathbf{x}_1, \mathbf{x}_2) = \langle[U(\mathbf{x}_1, \omega) - \overline{U}(\mathbf{x}_1)][U(\mathbf{x}_2, \omega) - \overline{U}(\mathbf{x}_2)]\rangle$. These statistical moments can be estimated from the field data. For example, for any two points $\mathbf{x}_1 = (x_{11}, x_{12}, x_{13})^T$ and $\mathbf{x}_2 = (x_{21}, x_{22}, x_{23})^T$ in domain D, the covariance function may take the separate exponential form

$$C_U(\mathbf{x}_1,\mathbf{x}_2)=\sigma_U^2\exp\left[-\sum_{i=1}^{3}\frac{|x_{1i}-x_{2i}|}{\lambda_i}\right], \tag{9}$$

or the Gaussian form

$$C_U(\mathbf{x}_1, \mathbf{x}_2) = \sigma_U^2 \exp\left[-\frac{\pi}{4}\sum_{i=1}^{3}\left(\frac{x_{1i}-x_{2i}}{\lambda_i}\right)^2\right]. \quad (10)$$

In the above, σ_U^2 is the variance, λ_i is the correlation length in the ith dimension. By definition, the covariance function is symmetric and positive definite, which means that it can be decomposed as [*Courant and Hilbert*, 1953]:

$$C_U(\mathbf{x}_1, \mathbf{x}_2) = \sum_{i=1}^{\infty} \eta_i \tilde{U}_i(\mathbf{x}_1)\tilde{U}_i(\mathbf{x}_2), \quad (11)$$

where η_i and $\tilde{U}_i(\mathbf{x})$ are the eigenvalues and eigenfunctions of the covariance function, respectively. They can be solved from the following Fredholm equation of second kind:

$$\int_D C_U(\mathbf{x}_1, \mathbf{x}_2)\tilde{U}_i(\mathbf{x}_2)d\mathbf{x}_2 = \eta_i \tilde{U}_i(\mathbf{x}_1). \quad (12)$$

Because of the symmetry and the positive definiteness of the covariance function, its eigenvalues are positive and real, and its eigenfunctions are orthogonal and form a complete set,

$$\int_D \tilde{U}_i(\mathbf{x})\tilde{U}_j(\mathbf{x})d\mathbf{x} = \delta_{ij}, \quad (13)$$

where δ_{ij} is the Kronecker delta function, which equals to one for $i = j$ and zero otherwise. Then the random field can be expressed as

$$U(\mathbf{x}, \omega) = \overline{U}(\mathbf{x}) + U'(\mathbf{x}, \omega) = \overline{U}(\mathbf{x}) + \sum_{i=1}^{\infty} \xi_i(\omega)\sqrt{\eta_i}\tilde{U}_i(\mathbf{x}), \quad (14)$$

where ξ_i are a set of orthogonal random variables satisfying $\langle \xi_i \rangle = 0$ and $\langle \xi_i \xi_j \rangle = \delta_{ij}$. When the underlying random field is Gaussian, ξ_i are independent, standard Gaussian random variables. The expansion in equation (14) is called the KL expansion. The random field $U(\mathbf{x}, \omega)$ is decomposed as the sum of its mean and a mean-removed part, which is further represented by a series of KL terms. Without loss of generality, it is assumed that the eigenvalues have been sorted in a nonincreasing order $\eta_1 \geq \eta_2 \geq \ldots$ and their corresponding eigenfunctions are also sorted accordingly. By truncating the infinite KL series at the Nth term, $U(\mathbf{x}, \omega)$ is approximated via N random variables ξ_i, $i = 1, \ldots, N$, weighted by the eigenvalues and deterministic eigenfunctions. When the underlying random field is Gaussian, this approximation is optimal with mean square convergence. For some particular covariance functions defining on regular domains (such as rectangular domains in 2-D), eigenvalues and eigenfunctions can be solved analytically [*Ghanem and Spanos*, 1991; *Zhang and Lu*, 2004]. However, in general, the integral equation (12) has to be solved numerically [*Ghanem and Spanos*, 1991].

[11] One of the interesting features of the KL expansion is that the sum of all eigenvalues is related to the total variability of the input field. Setting $\mathbf{x}_1 = \mathbf{x}_2 = \mathbf{x}$ in equation (11), integrating it over the domain D, and recalling orthogonality of the eigenfunctions yields

$$\int_D \sigma_U^2(\mathbf{x})d\mathbf{x} = \int_D C_U(\mathbf{x}, \mathbf{x})d\mathbf{x} = \int_D \left[\sum_{i=1}^{\infty} \eta_i U_i^2(\mathbf{x})\right]d\mathbf{x} = \sum_{i=1}^{\infty} \eta_i, \quad (15)$$

where $\sigma_U^2(\mathbf{x}) = C_U(\mathbf{x}, \mathbf{x})$ is the variance function of $U(\mathbf{x}, \omega)$. If $U(\mathbf{x}, \omega)$ is second-order stationary, (15) leads to $\sum_{i=1}^{\infty} \eta_i = |D|\sigma_U^2$, where $|D|$ is the measure of the domain D. Equation (15) indicates that the total variability of $U(\mathbf{x}, \omega)$ over the whole domain is distributed to all KL terms, with the weight of η_i. The KL decomposition can also be applied to nonstationary random fields due to conditioning on direct measurements [*Lu and Zhang*, 2004] or zonation [*Lu and Zhang*, 2007]. The KL decomposition is a spectral decomposition. As will be shown in the illustrative examples, different KL terms reflect the variability on different length scales. So the physical meaning of the KL expansion is to separate the uncertainty on different spatial scales. Thus we can effectively approximate the stochastic property of a random field with relatively few random variables, by retaining those leading KL terms (terms with large eigenvalues).

3.2. Multiple-Input Random Fields

[12] For many models, such as the case we will show in the illustrative examples, there could be more random parameters than only one. Consider multiple random fields defined on the same physical domain: U_i, $i = 1, 2, \ldots, M$. Their mean functions $\overline{U}_i(\mathbf{x}) = \langle U_i(\mathbf{x}, \omega) \rangle$ and covariance functions $C_{U_i}(\mathbf{x}_1, \mathbf{x}_2) = \langle [U_i(\mathbf{x}_1, \omega) - \overline{U}_i(\mathbf{x}_1)][U_i(\mathbf{x}_2, \omega) - \overline{U}_i(\mathbf{x}_2)] \rangle$ are prescribed. The correlations between these random fields are described by the correlation coefficients:

$$\gamma_{U_iU_j} = \frac{\langle [U_i(\mathbf{x}, \omega) - \overline{U}_i(\mathbf{x})][U_j(\mathbf{x}, \omega) - \overline{U}_j(\mathbf{x})] \rangle}{\sigma_{U_i}\sigma_{U_j}} \quad (16)$$

σ_{U_i} is the standard deviation of U_i and $\gamma_{U_iU_j} \in [-1, 1]$. U_i and U_j are perfectly correlated when $\gamma_{U_iU_j} = \pm 1$. $\gamma_{U_iU_j}(i, j = 1, 2, \ldots, M)$ form an M by M symmetric and positive definite matrix, which means that it can be decomposed into $\gamma_{U_iU_j} = \sum_{k=1}^{M} L_{ik}L_{jk}$ by Cholesky decomposition, where L_{ik} denotes an M by M lower triangular matrix. Furthermore, we have the KL decomposition,

$$C_{U_i}(\mathbf{x}_1, \mathbf{x}_2) = \sum_{m=1}^{\infty} \eta_m^i \tilde{U}_m^i(\mathbf{x}_1)\tilde{U}_m^i(\mathbf{x}_2), \quad (17)$$

where η_m^i and $\tilde{U}_m^i$ are the eigenvalues and the eigenfunctions of U_i, respectively. Then we can incorporate the correlation into the representation of the input random fields as the following

$$\begin{aligned} U_i(\mathbf{x}, \omega) &= \overline{U}_i(\mathbf{x}) + U_i'(\mathbf{x}, \omega) \\ &= \overline{U}_i(\mathbf{x}) + \sum_{m=1}^{\infty} \sqrt{\eta_m^i}\tilde{U}_m^i(\mathbf{x})\left(\sum_{k=1}^{M} L_{ik}\xi_{km}\right) \end{aligned} \quad (18)$$

where $\{\xi_{km}\}$ are independent Gaussian random variables. It can be shown that the KL representation (18) has the same mean and covariance functions as the prescribed input fields. By truncating the infinite summation in (18) at the Nth term, again, we can approximately represent the input random fields via $N \times M$ random variables $\{\xi_{11}, \xi_{12}, \ldots, \xi_{1N}, \xi_{21}, \ldots \xi_{2N}, \ldots, \xi_{M1}, \ldots \xi_{MN}\}$,

$$U_i(\mathbf{x},\omega) = \overline{U}_i(\mathbf{x}) + U_i'(\mathbf{x},\omega) = \overline{U}_i(\mathbf{x}) + \sum_{m=1}^{N} \sqrt{\eta_m^i}\, \tilde{U}^i_m(\mathbf{x}) \left(\sum_{k=1}^{M} L_{ik}\xi_{km} \right). \quad (19)$$

4. Representation of the Output Fields: Polynomial Chaos Expansion

4.1. General Formulation

[13] Because the output random field ψ or S_e depends on the input, it can be shown that ψ or S_e is a function of the random vector $\boldsymbol{\xi} = (\xi_1, \xi_2, \ldots, \xi_N)^T$, where ξ_i are the random variables used to approximate the input parameters. However, the specific relationship between the output random fields and $\boldsymbol{\xi}$ is yet to be determined.

[14] Since the statistics of the output random fields are not known in advance, ψ or S_e cannot be represented using the KL expansion. Alternatively, PCE is a more general representation for the output fields. In the following derivations, we take the pressure head as an example. The effective saturation can be expanded in a similar way. Suppose ψ can be expanded by a polynomial form:

$$\psi(\mathbf{x},t,\boldsymbol{\xi}) = a_0(\mathbf{x},t) + \sum_{i_1=1}^{\infty} a_{i_1}(\mathbf{x},t)\Gamma_1(\xi_{i_1}) + \sum_{i_1=1}^{\infty}\sum_{i_2=1}^{i_1} a_{i_1 i_2}(\mathbf{x},t)\Gamma_2(\xi_{i_1},\xi_{i_2}) + \sum_{i_1=1}^{\infty}\sum_{i_2=1}^{i_1}\sum_{i_3=1}^{i_2} a_{i_1 i_2 i_3}(\mathbf{x},t)\Gamma_3(\xi_{i_1},\xi_{i_2},\xi_{i_3}) + \ldots, \quad (20)$$

where $a_0(\mathbf{x}, t)$ and $a_{i_1 i_2 \ldots i_d}(\mathbf{x}, t)$ are deterministic coefficients. The basis $\Gamma_d(\xi_{i_1}, \ldots, \xi_{i_d})$ is a set of polynomial chaos with respect to those independent random variables $\xi_{i_1}, \ldots, \xi_{i_d}$ [*Wiener*, 1938]. For independent standard Gaussian random variables, $\Gamma_d(\xi_{i_1}, \ldots, \xi_{i_d})$ are the multidimensional Hermit polynomials with order of d. They are expressed as

$$\Gamma_d(\xi_{i_1},\ldots,\xi_{i_d}) = (-1)^d e^{\frac{1}{2}\boldsymbol{\xi}^T\boldsymbol{\xi}} \frac{\partial^d}{\partial\xi_{i_1}\ldots\partial\xi_{i_d}} \left(e^{\frac{1}{2}\boldsymbol{\xi}^T\boldsymbol{\xi}} \right), \quad (21)$$

where $\boldsymbol{\xi} = (\xi_{i_1}, \ldots, \xi_{i_d})^T$ [e.g., *Li and Zhang*, 2007]. By truncating the polynomial series in equation (20) at a certain order, we have an approximation of the output random field. In particular, the second-order approximation with Hermit polynomials can be written as

$$\hat{\psi}(\mathbf{x},t,\boldsymbol{\xi}) = a_0(\mathbf{x},t) + \sum_{i=1}^{N} a_i(\mathbf{x},t)\xi_i + \sum_{i=1}^{N} a_{ii}(\mathbf{x},t)\left(\xi_i^2 - 1\right) + \sum_{i=1}^{N}\sum_{j=1}^{i-1} a_{ij}(\mathbf{x},t)\xi_i\xi_j, \quad (22)$$

or a simplified form

$$\hat{\psi}(\mathbf{x},t,\boldsymbol{\xi}) = \sum_{j=1}^{P} c_j(\mathbf{x},t)\Phi_j(\boldsymbol{\xi}). \quad (23)$$

[15] There is a one-to-one correspondence between the terms in (22) and (23). For example, $\Phi_1(\boldsymbol{\xi}) = 1$, $\Phi_2(\boldsymbol{\xi}) = \xi_1$, and $\Phi_{N+2}(\boldsymbol{\xi}) = (\xi_1^2 - 1)$. The total number of PCE terms is $P = (N + d)!/(N!d!)$, where N is the random dimensionality (the number of KL terms retained to represent the mean-removed random input fields) and d is the order of polynomial chaos.

4.2. Leading Term Approximation

[16] As will be shown in section 5, the computational effort required to implement the PCM is regulated by the total number of terms retained in the PCE. However, this number P will increase significantly as the number (N) of terms kept in the truncated KL approximation grows. To avoid this burden, one may retain only those leading terms in the PCE approximation. For example, we may eliminate all the cross terms in (22),

$$\hat{\psi}(\mathbf{x},t,\boldsymbol{\xi}) = a_0(\mathbf{x},t) + \sum_{i=1}^{N} a_i(\mathbf{x},t)\xi_i + \sum_{i=1}^{N} a_{ii}(\mathbf{x},t)\left(\xi_i^2 - 1\right) \quad (24)$$

and the number of terms in the approximate polynomials is reduced to $P = 1 + 2N$.

4.3. Statistical Moments

[17] One of the important properties of the polynomial chaos is that all the polynomials in equation (23) are mutually orthogonal, which means $\langle \Phi_i(\boldsymbol{\xi})\Phi_j(\boldsymbol{\xi})\rangle = 0$ for $i \neq j$, and for $i = j$, $\langle \Phi_j^2 \rangle$ can be evaluated easily [*Ghanem and Spanos*, 1991]. Once the coefficients $c_j(\mathbf{x}, t)$ are determined, as described in section 5, the statistical properties of the flow quantities such as the pressure head and the effective saturation can be easily estimated from equation (23). For example, the mean pressure head is

$$\overline{\hat{\psi}}(\mathbf{x},t,\boldsymbol{\xi}) = \langle \hat{\psi}(\mathbf{x},t,\boldsymbol{\xi})\rangle = \sum_{j=1}^{P} c_j(\mathbf{x},t)\langle\Phi_j(\boldsymbol{\xi})\rangle = c_1(\mathbf{x},t). \quad (25)$$

Note that in deriving equation (25), we have used the following properties of the polynomial chaos: $\Phi_1(\boldsymbol{\xi}) = 1$,

and $\langle \Phi_j(\boldsymbol{\xi}) \rangle = \langle \Phi_j(\boldsymbol{\xi}) \Phi_1(\boldsymbol{\xi}) \rangle = 0$ for $j = 2, 3, \ldots P$. The variance of the pressure head is

$$\sigma^2_{\hat{\psi}} = \langle (\hat{\psi}(\mathbf{x}, t, \boldsymbol{\xi}) - \langle \hat{\psi}(\mathbf{x}, t, \boldsymbol{\xi}) \rangle)^2 \rangle = \sum_{j=2}^{P} \sum_{k=2}^{P} c_j(\mathbf{x}, t) c_k(\mathbf{x}, t) \langle \Phi_j(\boldsymbol{\xi}) \Phi_k(\boldsymbol{\xi}) \rangle = \sum_{j=2}^{P} c_j^2(\mathbf{x}, t) \langle \Phi_j^2 \rangle, \quad (26)$$

where $\langle \Phi_j^2 \rangle$ can be evaluated in advance. Higher statistical moments can be calculated similarly.

5. Probabilistic Collocation Method

[18] Galerkin's approach and Probabilistic Collocation Method (PCM) are two of the methods that may be used to determine the coefficients $c_j(\mathbf{x})$ in the polynomial expansion. Here we choose the PCM, which leads to independent equations and is thus capable of easily dealing with complex nonlinear problems.

5.1. Implementation of Probabilistic Collocation Method

[19] The probabilistic collocation method has no essential differences compared with the typical collocation method except that the typical collocation method is used to obtain a deterministic solution whereas the PCM is used to seek a random solution defined on probability space. Again, we only demonstrate how to determine the coefficients in the PCE approximation of the pressure head. The coefficients in the PCE approximation of the effective saturation can be determined similarly. Let $\psi = \psi(\mathbf{x}, t, \boldsymbol{\xi})$ denote the solution of the nonlinear stochastic differential equations. We seek an approximate solution as described in equation (23). We define the residual between the unknown solution $\psi(\mathbf{x}, t, \boldsymbol{\xi})$ and this approximation as

$$R_P(\mathbf{x}, t, \boldsymbol{\xi}) = \psi(\mathbf{x}, t, \boldsymbol{\xi}) - \hat{\psi}(\mathbf{x}, t, \boldsymbol{\xi}). \quad (27)$$

The collocation method proceeds by requiring this residual to vanish at some sets of collocation points $\boldsymbol{\xi}^1, \boldsymbol{\xi}^2, \ldots, \boldsymbol{\xi}^P$. The procedure is summarized as follows [*Li and Zhang*, 2007]:

[20] First, choose P collocation points in the probability space, $\boldsymbol{\xi}^i = (\xi_1^i, \xi_2^i, \ldots, \xi_N^i)^T$, $i = 1, 2, \ldots, P$, as described in section 5.2. Second, substitute $\boldsymbol{\xi}^i = (\xi_1^i, \xi_2^i, \ldots, \xi_N^i)^T$ into the KL expansion to generate a representation of the input field. For each of the P representations, the differential equations are deterministic and can be solved to give an output $\psi(\mathbf{x}, t, \boldsymbol{\xi}^i)$. This leads to P sets of independent equations that can be solved in parallel or in sequence. With the P sets of solutions and by letting $R_P(\mathbf{x}, t, \boldsymbol{\xi}^i) = 0$, one has

$$\sum_{j=1}^{P} c_j(\mathbf{x}, t) \Phi_j(\boldsymbol{\xi}^i) = \psi(\mathbf{x}, t, \boldsymbol{\xi}^i), \quad i = 1, 2, \ldots, P. \quad (28)$$

For each location $\mathbf{x}$ and time step t, the above equations form P linear equations for P unknowns $c_j(\mathbf{x}, t)$. The matrix of coefficients $\Phi_j(\boldsymbol{\xi}^i)$ are evaluated at the collocation point $\boldsymbol{\xi}^i$ and the right-hand sides $\psi(\mathbf{x}, t, \boldsymbol{\xi}^i)$ are solved from the original governing equation for the given collocation point in probability space. By solving this linear system, the coefficients in the PCE expansion can be determined for locations and time steps of interest.

[21] An alternate approach for determining the unknown coefficients is the Galerkin approach [*Ghanem and Spanos*, 1991]. In this approach, the residual is required to be orthogonal to the basis functions $\Phi_j(\boldsymbol{\xi})$ that are used in the PCE expansion,

$$\langle R_P(\mathbf{x}, t, \boldsymbol{\xi}) \Phi_j(\xi) \rangle = 0, \qquad j = 1, 2, \ldots, P. \quad (29)$$

Again, we have P constraints to determine the P unknown coefficients $c_j(\mathbf{x}, t)$. Note that equation (29) results in P coupled equations. Solving these coupled equations could be complicated and time-consuming, especially when one considers spatially varying coefficients (when the solution is not a random variable but a random field) or nonlinear problems. On the other hand, the PCM method leads to uncoupled equations, each of which can be solved with existing, deterministic simulators. This feature makes the PCM applicable to linear or nonlinear problems in a straightforward manner.

5.2. Selection of the Collocation Points

[22] One key issue in the PCM approach is the selection of collocation points. Previous studies have demonstrated that for a given order of the PCE approximation the coordinates of each collocation point should be selected from the roots of the next higher-order orthogonal polynomial. This technique, which is analogous to Gaussian quadrature, will yield the result that is much more accurate than the randomly selected samples [*Webster et al.*, 1996; *Tatang et al.*, 1997]. For the case of second-order Hermit PCE, the coordinates of collocation points are selected from the roots of the third-order Hermit polynomial: $\xi^3 - 3\xi$, i.e., $-\sqrt{3}$, 0, and $\sqrt{3}$. Then each collocation point is a combination of these three roots; two examples of the collocation points are $\boldsymbol{\xi}^1 = (\xi_1^1, \xi_2^1, \ldots, \xi_N^1)^T = (0, 0, \ldots, 0)^T$ and $\boldsymbol{\xi}^2 = (\xi_1^2, \xi_2^2, \ldots, \xi_N^2)^T = (\sqrt{3}, 0, \ldots, 0)^T$.

[23] The number of collocation points required is equal to the number of coefficients to be determined $P = (N + d)!/(N!d!)$, where N is the dimensionality of the probability space and d is the order of PCE approximation (2 in this case). However, the number of available points satisfying the preceding requirement, that is, the number of different combinations of $(d + 1)$ roots, is $M = (d + 1)^N$. Note that M is always larger than P, the number of points needed. As a result, we may select P best combinations out of M combinations in total. One may optimize the selection of the collocation points with the following consideration [*Li and Zhang*, 2007].

[24] 1. Keep as many points as possible in the region with a high probability density. Actually the probability density $\rho(\boldsymbol{\xi})$ is the weight in the integral for calculating the statistical moments.

$$\overline{\psi}(\mathbf{x}, t) = \int_{\Omega} \psi(\mathbf{x}, t, \boldsymbol{\xi}) \rho(\boldsymbol{\xi}) d\boldsymbol{\xi} \quad (30)$$

$$\sigma_\psi^2(\mathbf{x},t) = \int_\Omega (\psi(\mathbf{x},t,\boldsymbol{\xi}) - \langle\psi(\mathbf{x},t,\boldsymbol{\xi})\rangle)^2 \rho(\boldsymbol{\xi}) d\boldsymbol{\xi} \quad (31)$$

By setting $\hat{\psi}(\mathbf{x}, t, \boldsymbol{\xi}) = \psi(\mathbf{x}, t, \boldsymbol{\xi})$ at the region with a high probability density one can increase the accuracy of the estimated statistical moments. For instance, when $\xi_1, \xi_2, \ldots, \xi_N$ are N independent standard Gaussian random variables, the random point $\boldsymbol{\xi} = (\xi_1, \xi_2, \ldots, \xi_N)^T$ follows the following joint distribution:

$$\rho(\boldsymbol{\xi}) = (2\pi)^{N/2} \exp\left(-\frac{\boldsymbol{\xi}^T\boldsymbol{\xi}}{2}\right), \quad (32)$$

and this density function reaches the highest value at the origin point $\boldsymbol{\xi} = (0, 0, \ldots, 0)^T$, which corresponds to the mean parameter field. Therefore, this point is always kept. In addition, from (32) it is seen that in selecting these points one should keep as many zeros as possible in $\boldsymbol{\xi}$.

[25] 2. The matrix with its components $\Phi_j(\boldsymbol{\xi}^i)$ in equation (28) must have a full rank. Thus the equations are mutually independent and a unique solution can be obtained. To achieve this objective, one should first sort the available points in an order of decreasing probability density. For instance, the point $(0, 0, \ldots, 0)$ should be the first collocation point. Then, for the candidate of the $(i + 1)^{th}$ collocation point, the $(i + 1)^{th}$ row of matrix $\Phi_j(\boldsymbol{\xi}^i)$ must be linearly independent with the previous i rows. Otherwise, this candidate is abandoned and the point with the next highest probability density should be tested. For given (N, d), the sets of collocation points may be selected once and tabulated for other simulations.

[26] If both ψ and S_e are represented via the same basis polynomial chaos, the collocation points for computing these two output fields can be the same, which means that the computational effort for solving the statistical moments of the two output fields is almost the same as that for only one output field. For example, if both ψ and S_e are represented via the second-order Hermit polynomial chaos and the input random dimensionality is 10, each of the output fields will have $P = (10 + 2)!/(10!2!) = 66$ coefficients to be determined. We just choose 66 collocation points from the combinations of the roots of the third-order Hermit polynomial and solve the deterministic equations at these points, for pressure head and water content simultaneously, rather than select $2P$ collocation points and solve the deterministic equations $2P$ times, P for pressure and P for water content.

6. Illustrative Examples

[27] We consider unsaturated flow in a two-dimensional vertical cross section of size 3 by 3 m, discretized into 30×60 rectangular elements of 0.1 by 0.05 m. We specify a constant deterministic flux rate $Q = -0.005$ m/d at the upper boundary (negative value standing for infiltration), a constant deterministic pressure head $\psi = 0$ (water table) at the bottom, and no flow at the left and right boundaries. The saturated and residual water content are $\theta_s = 0.4$ and $\theta_r = 0.01$, respectively.

[28] Note that both K_s and α are positive quantities and n is always larger than one. Here we assume that the log saturated hydraulic conductivity $f = \ln(K_s)$, the log pore size distribution parameter $\beta = \ln(\alpha)$ and the fitting parameter $s = \ln(n - 1)$ are second-order stationary Gaussian random fields with mean $\langle U\rangle$ and separate exponential covariance $C_U(\mathbf{x}_1, \mathbf{x}_2) = \sigma_U^2 \exp\left[-\sum_{i=1}^{2} \frac{|x_{1i} - x_{2i}|}{\lambda_{Ui}}\right]$, where $U = f, \beta, s$; σ_U^2 is the variance, λ_U is the correlation length of U. The subscripts $i = 1, 2$ refer to the vertical and horizontal dimensions, respectively. The variability of a parameter can also be given in terms of the coefficient of variation $CV_V = \sigma_V/\langle V\rangle$, for $V = K_s, \alpha, (n - 1)$. The mean values of the three input parameters are set to be $\langle K_s\rangle = 1m/d$, $\langle\alpha\rangle = 2m^{-1}$, and $\langle n\rangle = 1.4$. With the known mean and the coefficient of variation of a lognormal random field V, the moments of the corresponding normal random field $U = \ln V$ can be easily calculated via following relations [e.g., *Zhang*, 2002]:

$$\langle U\rangle = 2\ln\langle V\rangle - 0.5\ln\left[\langle V\rangle^2\left(1 + CV_V^2\right)\right], \quad (33)$$

$$\sigma_U^2 = \ln\left[1 + CV_V^2\right], \quad (34)$$

or conversely,

$$\langle V\rangle = \exp\left[\langle U\rangle + 0.5\sigma_U^2\right], \quad (35)$$

$$\sigma_V^2 = \left[\exp\left(\sigma_U^2\right) - 1\right]\exp\left[2\langle U\rangle + \sigma_U^2\right]. \quad (36)$$

[29] We design a series of model cases with different model complexity (steady flow with single-input random field, cases 1–4; steady flow with multiple-input random fields, case 5; transient flow with multiple-input random fields, case 5). For each case, we first derive the statistical moments (mean and variance) of output fields using the Probabilistic Collocation Method (PCM). For the purpose of comparison, we conduct Monte Carlo (MC) simulations with a large number of realizations. For each single run of Monte Carlo or PCM simulations, the FEHM code [*Zyvoloski et al.*, 1997] is used to solve the deterministic differential equations. Unless otherwise noted, the comparison of results from the MC method and the PCM is illustrated only along the central vertical line ($x_2 = 1.5$ m). In case 1, we demonstrate the calculated statistical moments of both the pressure head and the effective saturation. In other cases, only the results of pressure head are shown for the sake of succinctness.

6.1. Single Random Input

[30] In the first four cases of steady flow, we treat α and n to be deterministic but $f = \ln(K_s)$ as the only input random field with different levels of variability and different correlation lengths as shown in Table 1. These cases are designed to explore the impact of the input variability and the correlation length on the accuracy and efficiency of the PCM. As described previously, we decompose $f = \ln(K_s)$ using the KL expansion and retain the first N random terms: $f(\mathbf{x}, \omega) = \bar{f}(\mathbf{x}) + \sum_{i=1}^{N} \xi_{fi}(\omega)\sqrt{\eta_{fi}}\tilde{f}_i(\mathbf{x})$. The output random fields, the pressure head and the water content, can be written as $\psi = \psi(\mathbf{x}, \xi_{f1}, \xi_{f2}, \ldots, \xi_{fN})$ and $S_e = S_e(\mathbf{x}, \xi_{f1}, \xi_{f2}, \ldots, \xi_{fN})$,

Table 1. Summary of the Parameters in All Illustrative Cases

Cases	$\langle K_s \rangle$ (m/d)	CV_{Ks} (%)	λ_{fx} (m)	λ_{fy} (m)	$\langle \alpha \rangle$ (1/m)	CV_{α} (%)	$\lambda_{\beta x}$ (m)	$\lambda_{\beta y}$ (m)	$\langle n \rangle$	$CV_{(n-1)}$ (%)	λ_{sx} (m)	λ_{sy} (m)	Random Dimensionality
1	1	100	1	1	2	0	NA	NA	1.4	0	NA	NA	20
2	1	50	1	1	2	0	NA	NA	1.4	0	NA	NA	20
3	1	100	0.5	0.5	2	0	NA	NA	1.4	0	NA	NA	20
4	1	100	0.5	0.5	2	0	NA	NA	1.4	0	NA	NA	30
5	1	100	0.6	0.3	2	20	0.6	0.3	1.4	10	0.6	0.3	50 + 50 + 50 = 150

respectively, indicating that the dimensionality in the probability space is N.

[31] The contours of some selected eigenfunctions in case 1 are plotted in Figure 1. It is shown that the first eigenfunction represents the spatial variability on the large scale and the subsequent eigenfunctions represent the spatial variability on smaller scales. The eigenvalues and their summation for cases 1 and 3 are shown in Figure 2. A decaying trend of eigenvalues can be observed, which suggests that more input variability is distributed on large spatial scales. The decaying rate of eigenvalues depends on the correlation length relative to the domain size. The eigenvalues in case 1 decay faster than those in case 3, where the correlation scale is smaller. In the first three cases, we keep 20 terms in the KL expansion and use the second-order PCE. Under these conditions, 231(= 22!/20!/2!) times of simulations are needed. For comparison, we explore the convergence of MC simulations based on simulations up to

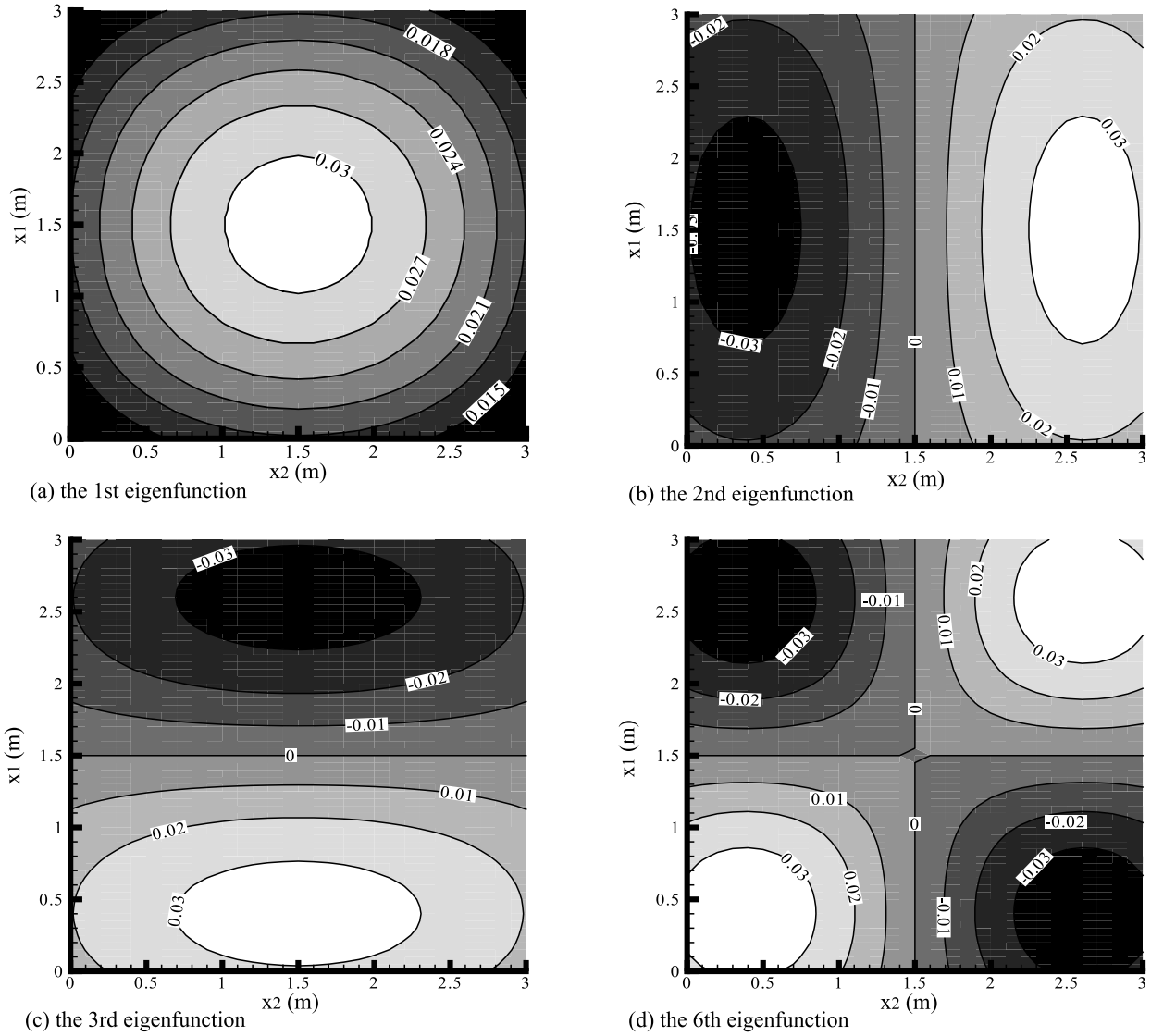

Figure 1. Selected eigenfunctions for case 1 ($\lambda_x = \lambda_y = 1.0m$).

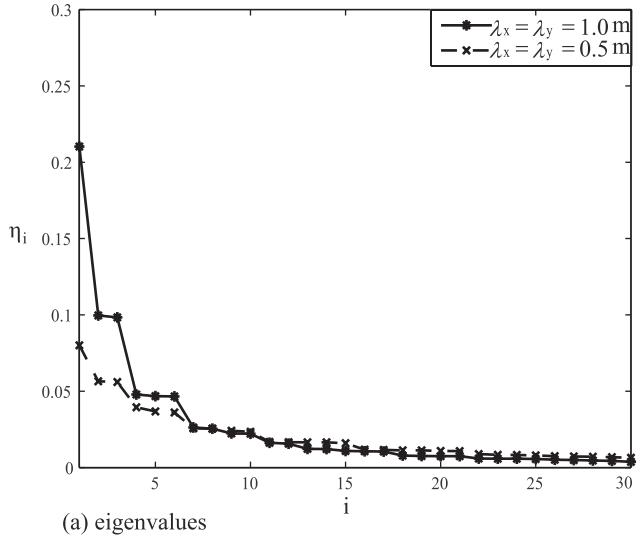

(a) eigenvalues

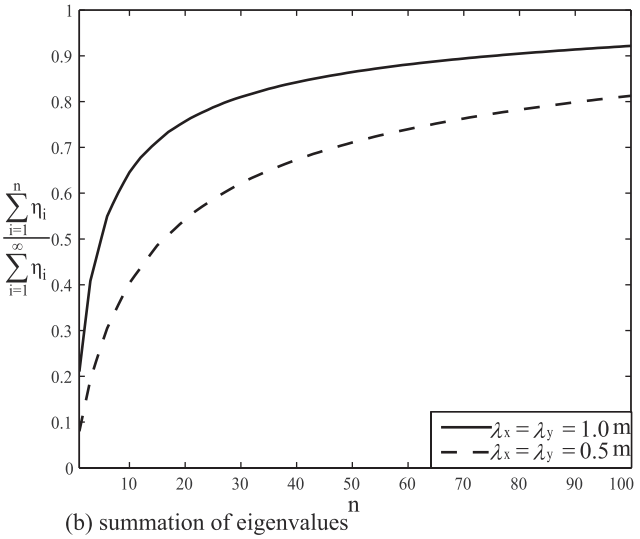

(b) summation of eigenvalues

Figure 2. Eigenvalues of the separate exponential covariance with different correlation scales.

8000 realizations. In particular, we are interested in the accuracy of MC results from 231 realizations, which represent the more or less equivalent computational cost required by the PCM. The statistical moments computed from all 8000 MC realizations are considered to be the "true" solutions for assessing the accuracy of the PCM. The mean and variance of pressure head and effective saturation from case 1 are plotted in Figure 3. First, from the results, we observe that the PCM solutions are in good agreement with those from 8000 MC simulations. However, the MC results computed from 231 realizations deviate substantially from the MC results from 8000 realizations ("true" solutions). As shown in Figure 4, for the mean pressure head, about 2000 MC simulations are needed to obtain the convergent result in this example while for the pressure head variance, about 4000 MC simulations are necessary to yield a convergent result. Since the computational efforts for 231 PCM simulations are more or less the same as those for 231 MC simulations, the comparison indicates that the PCM is computationally more efficient than the MC simulations. Second, the pressure head variance from the PCM is symmetric with respect to the vertical central line (shown in Figure 5), which is consistent with the symmetric boundary conditions on the left and right boundaries. For the MC approach, the symmetry of the pressure variance can be achieved only when a large number of simulations are conducted.

[32] We also compute the statistical moments of pressure head in case 1 with a reduced form of PCE as shown in equation (24). Under this condition, only 41(= 1 + 2 × 20) times of simulations are required. The result is added to Figures 3a and 3b. It reveals that the leading term strategy gives accurate solution with a much less computational effort. Furthermore, it is observed that the profiles of the curves in Figures 3a and 3b are quite similar to that in Figures 3c and 3d. This is because the effective saturation is directly dependent on the pressure head. At the upper part of the domain, a lower-pressure head leads to a lower water content and a large variability in the water content is consistent with a large variability in the pressure head.

[33] Figure 6 compares the pressure head variance derived from both the MC method and the PCM for different degrees of conductivity variability and two different correlation lengths. In cases 1 and 2, all input parameters are the same, except that the conductivity variability in case 2 is smaller than that in case 1. It is seen from Figure 6 that the PCM is more accurate when the conductivity variability is smaller. In cases 1 and 3, all input parameters are the same, except that the correlation length of the input random field in case 3 is smaller than that in case 1. Figure 6 indicates that the accuracy of the PCM decreases with the decrease of the correlation length. The reason is that the accuracy of the truncated KL expansion depends on the ratio of the domain size and the correlation length. It has been shown that, for a small correlation length, more terms are needed in the truncated KL expansion to retain the same accuracy [*Ghanem and Spanos*, 1991; *Zhang and Lu*, 2004]. We also run case 4 in which all the input parameters are the same as those in case 3 but the number of retained KL terms is 30. Under this condition, 496 simulations are required to implement the second-order PCM approach. It can be seen that when more terms are included in the truncated KL expansion, the results from the PCM are closer to the reference MC results.

6.2. Multiple-Input Random Fields

[34] One of the advantages of the PCM is the ease in dealing with multiple-input random parameters. In the next illustrative case (case 5), we make the following assumptions which are closer to the real-world conditions: (1) All the three soil parameters in the van Genuchten model ($U = f$, β, s) are assumed to be random fields and (2) they are partially correlated: f and β are positively correlated and they are both negatively correlated with s. These assumptions are consistent with previous experiments [*Russo and Bouton*, 1992; *Simunek et al.*, 1998].

6.2.1. Steady Flow

[35] We first calculate the steady state flow under the boundary conditions given in the previous cases. We assume the correlation coefficients between the three random parameters are: $\gamma_{f\beta} = 0.8$, $\gamma_{fs} = -0.3$, $\gamma_{\beta s} = -0.6$. The statistical properties of the input random fields are given in Table 1. We represent the three random fields as described

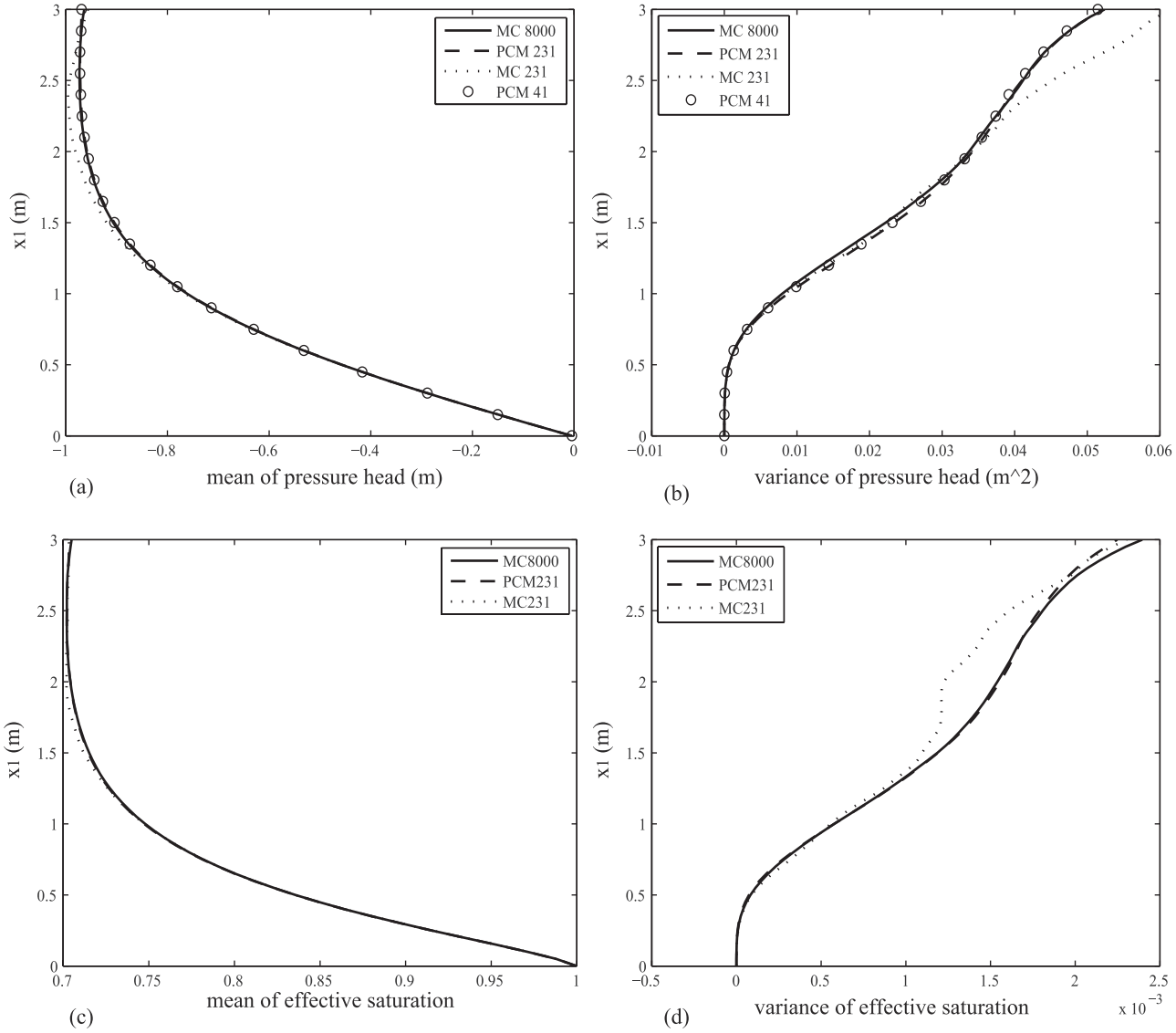

Figure 3. Comparison of results from MC and PCM methods for case 1 (CV_{Ks} = 100%, $\lambda_x = \lambda_y = 1.0m$) along the vertical central line.

in equation (18). Because of the small correlation length, we keep N = 50 KL terms in the representation of each input random field. Thus the total random dimensionality is $3N$ = 150. For such a high-dimensional problem, a full 2nd order PCE expansion of the output field would contain too many terms (P = (150 + 2)!/150!/2! = 11476) and the computational cost for determining all the coefficients will make the PCM approach not practical. Under this condition, the "leading term approximation" strategy described in section 4.2 is adopted. The total number of terms is reduced to P = 1 + 2 × (3N) = 301. The mean and variance of pressure derived from both the PCM and MC are compared along the central vertical profile, as shown in Figure 7. It is seen that the results given by the two approaches are in good agreement, which proves the capability of the PCM in quantifying the model uncertainty induced by multiple random inputs. Furthermore, it is reflected that the leading term approximation is applicable for this problem. From the results, we can also give some qualitative analysis of the distribution of the pressure. First, at the bottom portion (the portion right above the water table), the mean pressure linearly decreases with respect to the elevation, with a slope near −1. Hence the vertical gradient of the total head $\psi + x_1$ is very small at the bottom portion, compared with the top portion. This is because the saturation near the water table is much larger than in the regions far from it. So a small gradient in this portion is enough to induce the same flow rate as in the top portion. On the other hand, the mean pressure finally reaches a constant as the elevation increases to the upper boundary, which reveals that the flow is mainly driven by the gravity. Second, we can observe that the variance of the pressure head is zero near water table. This is consistent with the constant pressure boundary condition we assigned at the lower boundary. For the upper boundary, there is not such a constraint. The variance of pressure continually grows as the elevation increases and reaches the maximum at the upper boundary. This indicates that the flow in the "gravity dominated zone" can be the most affected by the variability of soil properties.

6.2.2. Transient Flow

[36] Finally, we test the capability of the PCM approach in dealing with transient problems. Following the last

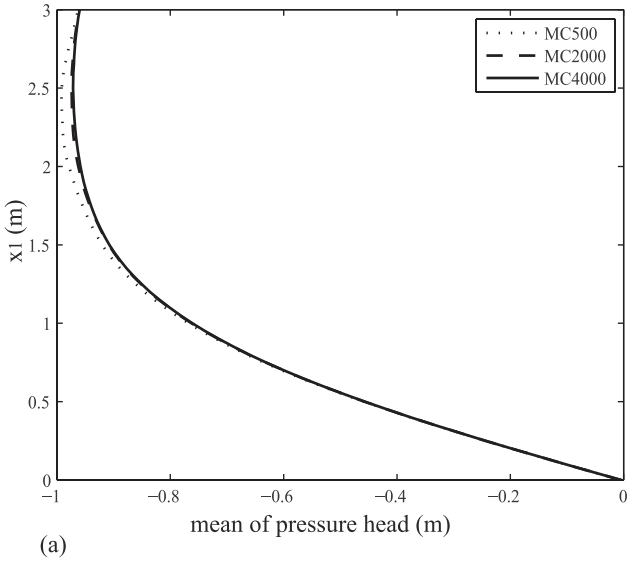

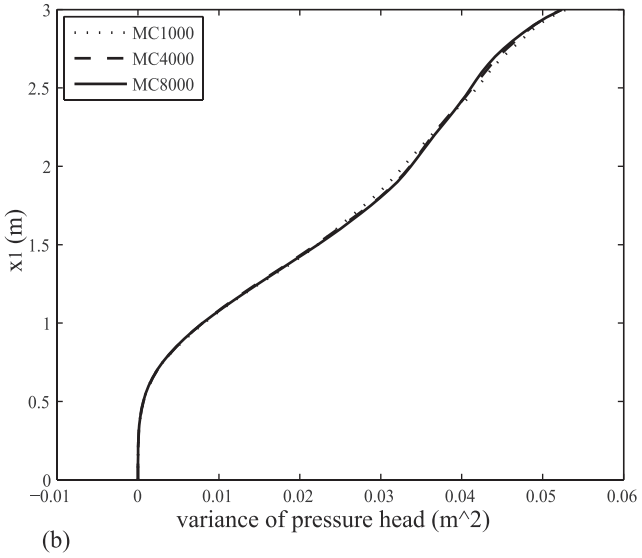

Figure 4. Mean and variance given by MC with different numbers of simulations (case 1).

example, we use the steady state solution (see Figure 7) as the initial condition and assume that the flow rate at the upper boundary changes from −0.005 m/d to −0.003 m/d at time t = 0 days. The transient process in the following time steps is simulated. The statistical moments of the pressure head after 3 and 15 days given by both the PCM and MC are plotted in Figure 8. Again, it is shown that the results given by the PCM and MC are in excellent agreement. By comparing the means of pressure head at the three time steps (t = 0, t = 3 and t = 15 days), we can observe the decreasing trend of pressure head, induced by the reducing of flow rate at the upper boundary. The pressure at the top portion changes first, and the middle portion follows, while the pressure at the bottom portion keeps unchanged. This reveals that the pressure distribution at the top portion is more sensitive to the infiltration rate than the lower portion. As time approaches, a new steady state is reached. On the other hand, the variance of the pressure changes only slightly as time approaches, which suggests that the uncertainty

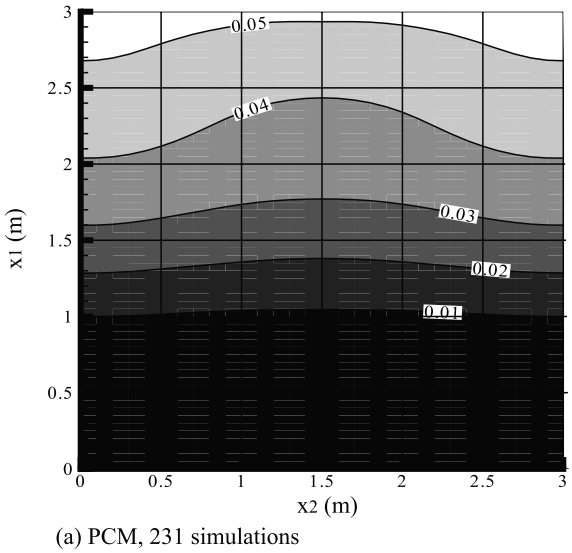

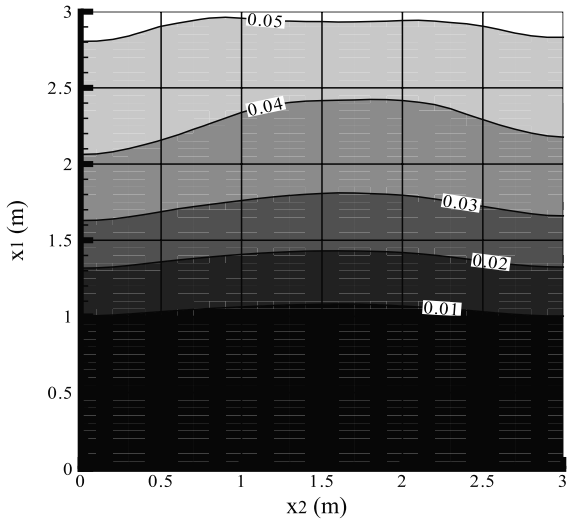

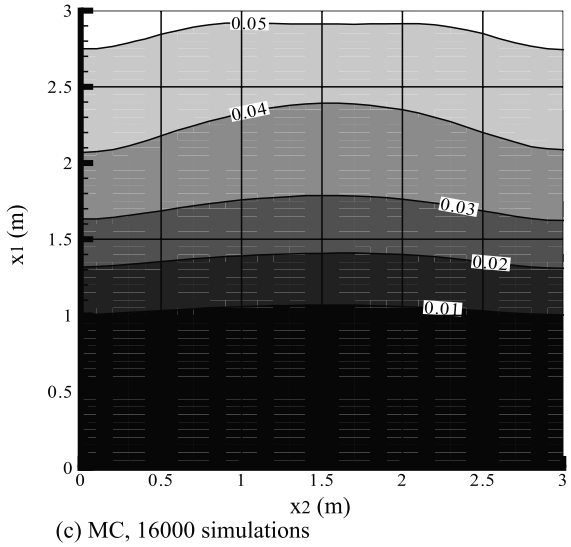

Figure 5. Contours of the pressure variance (m^2) in case 1.

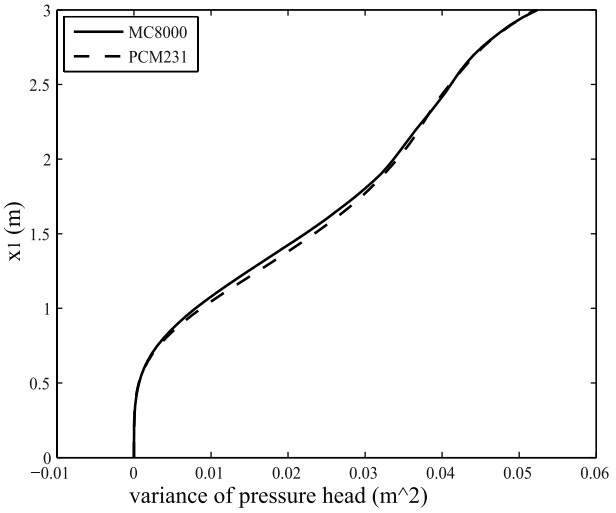

(a) case1. CV_{Ks}= 100% $\lambda_x = \lambda_y = 1.0$ m

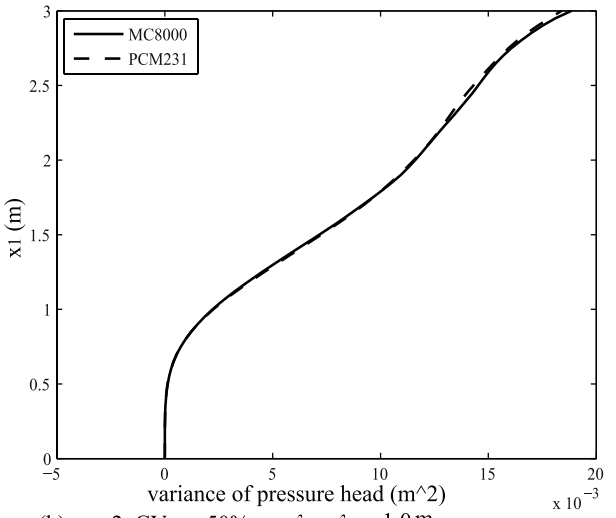

(b) case2. CV_{Ks}= 50% $\lambda_x = \lambda_y = 1.0$ m

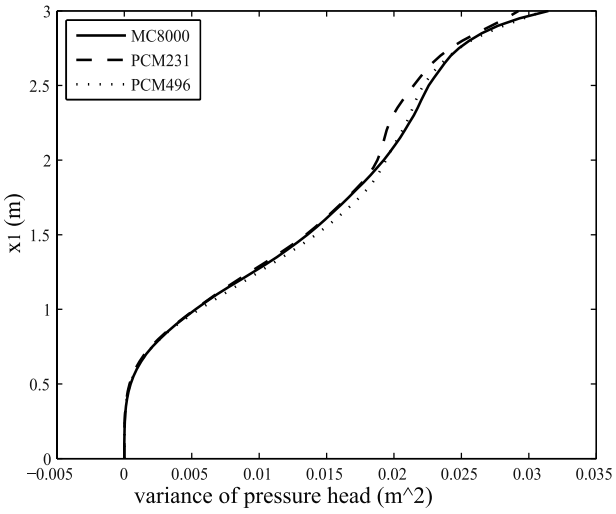

(c) case3 and 4. CV_{Ks} = 100% $\lambda_x = \lambda_y = 0.5$ m

Figure 6. Comparison of pressure variance derived from PCM and MC with different input variances and different correlation lengths (cases 1, 2, 3, and 4).

associated with the pressure distribution is not as sensitive to the flow rate as the mean pressure is.

7. Discussions and Conclusions

[37] Although the stochastic equations describing flow in the unsaturated zone is complex because of the nonlinearity, in this study we demonstrated that the Probability Collocation Method (PCM) is still applicable. Like the MC method, the PCM is based on solving a set of deterministic equations. The difference between two approaches is that the PCM requires the solutions at a set of selected collocation points whereas the MC requires the solutions at random sampling points. Both approaches can be implemented straightforwardly with the availability of a deterministic simulator. Like the MC, the PCM can be applied to various problems, either linear or nonlinear, either with single or multiple inputs.

[38] Because the stochastic structures of both input and output random fields have been carefully considered, the

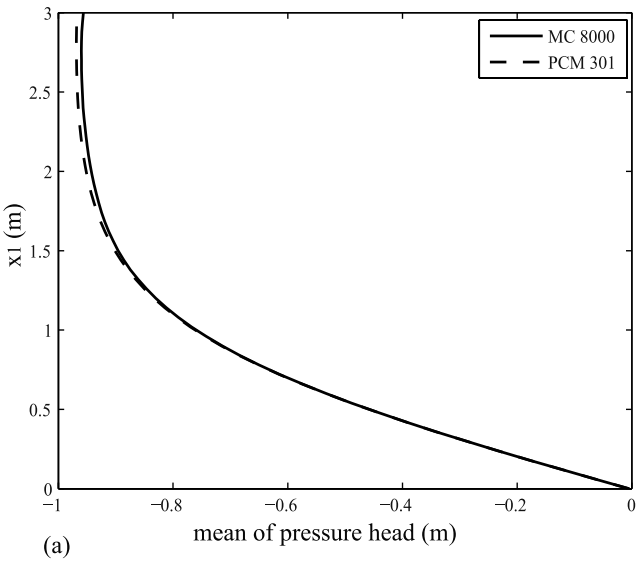

(a)

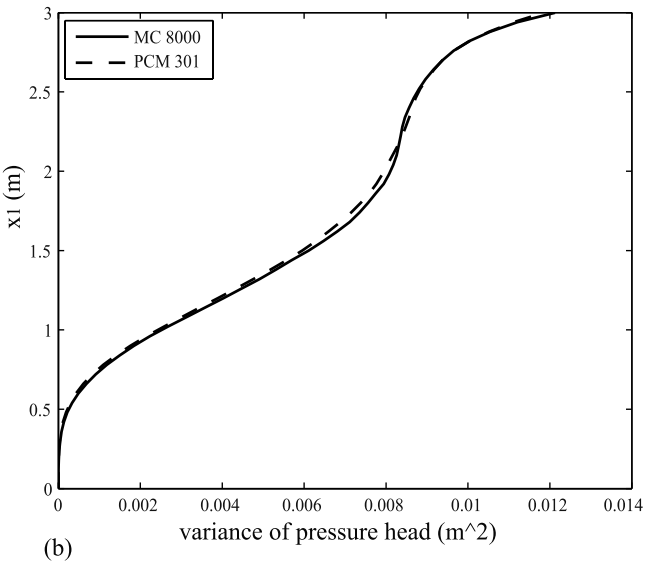

(b)

Figure 7. Statistics of pressure head with three mutually correlated input fields (case 5).

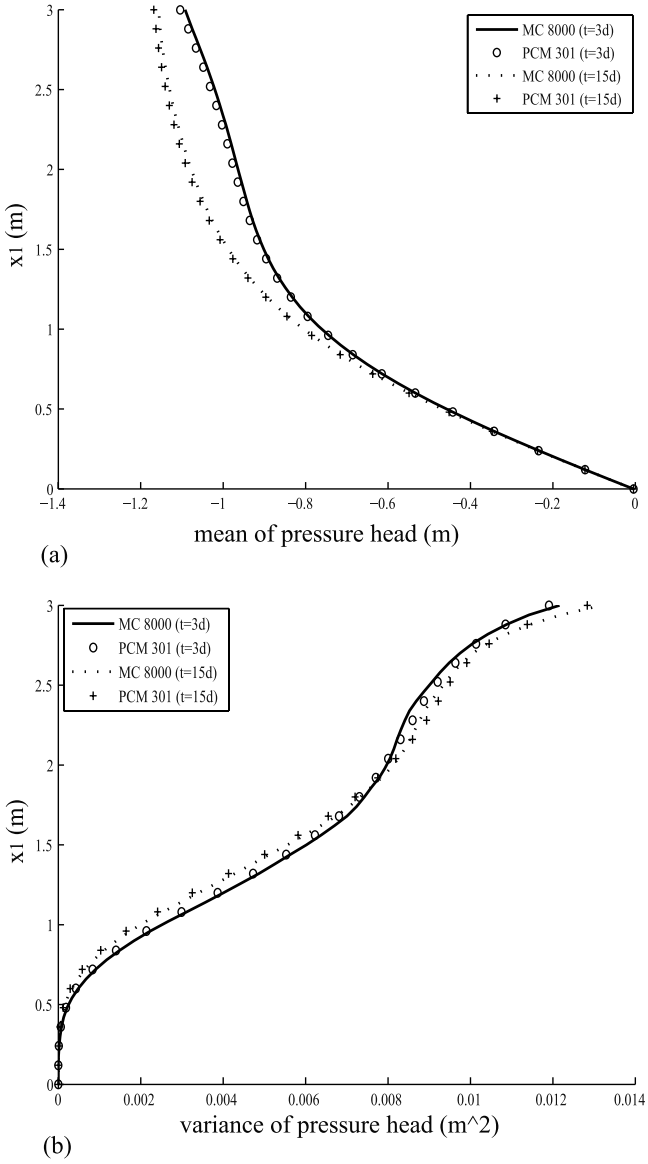

Figure 8. Statistics of pressure head at 3 and 15 days after the change of the flow rate (case 6).

PCM can capture the stochastic behavior of the dependent variables such as the pressure field and the effective saturation by a small number of model simulations. Hence the efficiency of the PCM is significantly increased compared to the MC. This advantage is crucial in solving large-scale problems because solving each deterministic equation may require a large computational effort.

[39] As shown in the illustrative examples, the PCM performs better when the input correlation scale is relatively large and the input variance is relatively small. If the correlation scale is too small or the input variance is too large, the PCM may yield inaccurate results. Actually, the truncations in the KL and PCE approximations are two major sources of errors in the PCM procedures, and the accuracy of KL and PCE approximations depend on the input correlation length and input variance, respectively. Our ongoing research attempts to derive posterior error estimators, which may be used to determine the proper random dimensionality of the KL expansions and the optimal order of PCE approximations to balance the solution accuracy and computational efficiency.

Notation

B Specific moisture capacity
C Covariance function
CV Coefficient of variation
c_j Coefficient of the jth PCE term
D Physical domain
d Order of polynomial chaos
f $f = \ln(K_s)$, log saturated hydraulic conductivity
g Sink/source term
H_B Prescribed pressure head-on Dirichlet boundary segments
K Unsaturated hydraulic conductivity
K_s Saturated hydraulic conductivity
m Fitting parameter in the van Genuchten-Mualem model
N Random dimensionality (Number of KL terms retained to represent the mean-removed fields)
n Fitting parameter in the van Genuchten-Mualem model
P Number of PCE terms
Q Prescribed specific discharge on Neumann boundary segments
$\mathbf{q}$ Specific discharge
R_P Residual between the true solution and PCE approximation with P terms
S_e Effective saturation
s $s = \ln(n - 1)$
U Normal random input field ($U = f, \beta, s$)
V Lognormal random input field ($V = K_s, \alpha, (n - 1)$)
$\mathbf{x}$ Cartesian coordinates in the physical domain
x_1 Elevation
α Fitting parameter in the van Genuchten-Mualem model
β $\beta = \ln(\alpha)$
Φ_j Hermit polynomials
Γ_D Dirichlet boundary
Γ_N Neumann boundary
η_i Eigenvalues
λ Correlation length
θ_e Effective water content
θ_r Residual water content
θ_s Saturated water content
ρ Probability density
σ^2 Variance
Ω Probability space
ω Point in the probability space
$\boldsymbol{\xi}$ Collocation point
ξ_i Orthogonal standard Gaussian random variables
ψ Pressure head
$\hat{\psi}$ PCE approximation of the pressure head

[40] **Acknowledgments.** This work is partially funded by National Science Foundation through grant DMS-0801425, the National Natural Science Foundation of China through grant 50688901, and the Chinese National Basic Research Program through grant 2006CB705800.

References

Brooks, R. H., and A. T. Corey (1964), Hydraulic properties of porous media, *Hydrol. Pap. 3*, Colo. State Univ., Fort Collins.

Chang, H., and D. Zhang (2009), A comparative study of stochastic collocation methods for flow in spatially correlated random fields, *Commun. Comput. Phys.*, *6*, 509–535.

Courant, R., and D. Hilbert (1953), *Methods of Mathematical Physics*, Interscience, New York.

Gardner, W. R. (1958), Some steady state solutions of unsaturated moisture flow equations with application to evaporation from a water table, *Soil Sci.*, *85*, 228–232.

Ghanem, R., and P. Spanos (1991), *Stochastic Finite Element: A Spectral Approach*, Springer, New York.

Jury, W. A. (1982), Simulation of solute transport using a transfer function model, *Water Resour. Res.*, *18*, 363–368, doi:10.1029/WR018i002p00363.

Li, H., and D. Zhang (2007), Probabilistic collocation method for flow in porous media: Comparisons with other stochastic methods, *Water Resour. Res.*, *43*, W09409, doi:10.1029/2006WR005673.

Li, H., and D. Zhang (2009), Efficient and accurate quantification of uncertainty for multiphase flow with probabilistic collocation method, *SPE J.*, in press.

Lu, Z., and D. Zhang (2002), Stochastic analysis of transient flow in heterogeneous, variably saturated porous media: The van Genuchten–Mualem constitutive model, *Vadose Zone J.*, *1*, 137–149, doi:10.2113/1.1.137.

Lu, Z., and D. Zhang (2004), Conditional simulations of flow in randomly heterogeneous porous media using a KL-based moment-equation approach, *Adv. Water Resour.*, *27*(9), 859–874, doi:10.1016/j.advwatres.2004.08.001.

Lu, Z., and D. Zhang (2007), Stochastic simulations for flow in nonstationary randomly heterogeneous media using a Karhunen-Loeve based moment-equation approach, *Multiscale Model. Simul.*, *6*(1), 228–245, doi:10.1137/060665282.

Mantoglou, A. (1992), A theoretical approach for modeling unsaturated flow in spatially variable soils: Effective flow models in finite domains and nonstationarity, *Water Resour. Res.*, *28*(1), 251–267, doi:10.1029/91WR02232.

Mantoglou, A., and L. Gelhar (1987), Stochastic modeling of large-scale transient unsaturated flow systems, *Water Resour. Res.*, *23*(1), 37–46, doi:10.1029/WR023i001p00037.

Russo, D. (1988), Determining soil hydraulic properties by parameter estimation: On the selection of a model for the hydraulic properties, *Water Resour. Res.*, *24*(3), 453–459, doi:10.1029/WR024i003p00453.

Russo, D. (1993), Stochastic modeling of macrodispersion for solute transport in a heterogeneous unsaturated porous formation, *Water Resour. Res.*, *29*(2), 383–397, doi:10.1029/92WR01957.

Russo, D. (1995), On the velocity covariance and transport modeling in heterogeneous anisotropic porous formations: 2. Unsaturated flow, *Water Resour. Res.*, *31*(1), 139–145, doi:10.1029/94WR01784.

Russo, D., and M. Bouton (1992), Statistical analysis of spatial variability in unsaturated flow parameters, *Water Resour. Res.*, *28*, 1911–1925, doi:10.1029/92WR00669.

Simunek, J., O. Wendroth, and M. T. van Genuchten (1998), Parameter estimation analysis of the evaporation method for determining soil hydraulic properties, *Soil Sci. Soc. Am. J.*, *62*, 894–905.

Tartakovsky, D. M., S. P. Neuman, and Z. Lu (1999), Conditional stochastic averaging of steady state unsaturated flow by means of Kirchhoff transformation, *Water Resour. Res.*, *35*, 731–745, doi:10.1029/1998WR900092.

Tatang, M. A., W. Pan, R. G. Prinn, and G. J. McRae (1997), An efficient method for parametric uncertainty analysis of numerical geophysical models, *J. Geophys. Res.*, *102*(D18), 21,925–21,931, doi:10.1029/97JD01654.

van Genuchten, M. T. (1980), A closed-form equation for predicting the hydraulic conductivity of unsaturated soils, *Soil Sci. Soc. Am. J.*, *44*, 892–898.

Webster, M., M. A. Tatang, and G. J. Mcrae (1996), Application of the probabilistic collocation method for an uncertainty analysis of a simple ocean model, *MIT Jt. Program on the Sci. and Policy of Global Change Rep.Ser., 4*, Mass. Inst. of Technol., Cambridge.

Wiener, N. (1938), The homogeneous chaos, *Am. J. Math.*, *60*, 897–936, doi:10.2307/2371268.

Yang, J., D. Zhang, and Z. Lu (2004), Stochastic analysis of saturated-unsaturated flow in heterogeneous media by combining Karhunen-Loeve expansion and perturbation method, *J. Hydrol.*, *294*, 18–38, doi:10.1016/j.jhydrol.2003.10.023.

Yeh, T.-C., L. W. Gelhar, and A. L. Gutjahr (1985a), Stochastic analysis of unsaturated flow in heterogeneous soils: 1. Statistically isotropic media, *Water Resour. Res.*, *21*(4), 447–456, doi:10.1029/WR021i004p00447.

Yeh, T.-C., L. W. Gelhar, and A. L. Gutjahr (1985b), Stochastic analysis of unsaturated flow in heterogeneous soils: 2. Statistically anisotropic media with variable α, *Water Resour. Res.*, *21*(4), 457–464, doi:10.1029/WR021i004p00457.

Zhang, D. (1999), Nonstationary stochastic analysis of transient unsaturated flow in randomly heterogeneous media, *Water Resour. Res.*, *35*(4), 1127–1141, doi:10.1029/1998WR900126.

Zhang, D. (2002), *Stochastic Methods for Flow in Porous Media: Coping With Uncertainties*, Academic, San Diego, Calif.

Zhang, D., and C. L. Winter (1998), Nonstationary stochastic analysis of steady state flow through variably saturated, heterogeneous media, *Water Resour. Res.*, *34*(5), 1091–1100, doi:10.1029/97WR03661.

Zhang, D., and Z. Lu (2004), An efficient, high-order perturbation approach for flow in random porous media via Karhunen-Loeve and polynomial expansions, *J. Comput. Phys.*, *194*(2), 773–794.

Zyvoloski, G. A., B. A. Robinson, Z. V. Dash, and L. L. Trease (1997), Summary of the models and methods for the FEHM application—A finite-element heat- and mass-transfer code, *Rep. LA-13307-MS*, Los Alamos Natl. Lab., Los Alamos, N. M.

W. Li, Department of Energy and Resources Engineering, College of Engineering, Peking University, Beijing 100871, China. (weixuan@pku.edu.cn)

Z. Lu, Earth and Environmental Sciences Division, Los Alamos National Laboratory, Los Alamos, NM 87545, USA. (zhiming@lanl.gov)

D. Zhang, Sonny Astani Department of Civil and Environmental Engineering, University of Southern California, Kaprelian Hall, 238B, 3620 South Vermont Avenue, Los Angeles, CA 90089, USA. (donzhang@usc.edu)